Spectra of sparse regular graphs with loops

F. L. Metz[1], I. Neri[2,3], and D. Bollé[1]

[1]*Instituut voor Theoretische Fysica, Katholieke Universiteit Leuven, Celestijnenlaan 200D, B-3001 Leuven, Belgium*
[2]*Université Montpellier 2, Laboratoire Charles Coulomb UMR 5221, F-34095, Montpellier, France*
[3]*CNRS, Laboratoire Charles Coulomb UMR 5221, F-34095, Montpellier, France*

We derive exact equations that determine the spectra of undirected and directed sparsely connected regular graphs containing loops of arbitrary length. The implications of our results to the structural and dynamical properties of networks are discussed by showing how loops influence the size of the spectral gap and the propensity for synchronization. Analytical formulas for the spectrum are obtained for specific length of the loops.

Networks have emerged as a unified framework to study complex problems in disciplines ranging from physics, biology, information theory, chemistry to technological and social sciences [1]. Some notable examples are the backbone of the Internet, which consists of routers connected by physical links, and the metabolism of the cell, represented as a tripartite network of metabolites, reactions and enzymes. As many seemingly unrelated problems are modeled by networks, it is crucial to understand how the topology of networks influences the processes governed on them. The efficiency of error-correcting codes and communication networks [2, 3], the propensity for synchronization [4, 5] and the mixing times of search algorithms [6], among others, are unveiled from a spectral analysis, i.e. from a study of the adjacency matrix and the Laplacian of the network [7].

A widespread theoretical approach consists in modeling real-world networks by sparsely connected random graphs [8], which have a local tree-like structure and thus a small number of short loops. The *Kesten-McKay law* [9] for the spectrum of sparse regular graphs is a rare example of an analytical solution for the spectral density and shows that regular graphs have a large spectral gap, implying many optimal structural properties [3]. Spectral analyzes of irregular sparse random graphs such as Erdös-Rényi graphs [10, 11], scale-free graphs and small-world systems have recently been considered [12].

However, Bravais lattices and real-world networks, such as the Internet and metabolic networks, exhibit a large number of undirected and directed short loops [13], while other examples like power grids and neural networks are under-short looped, i.e. they have less short loops than their corresponding random graph models [14]. To study the effect of loops on structural and dynamical properties of complex networks we consider the *Husimi graph* [15] (also called Husimi cactus), which is built out of randomly drawn short loops. The Husimi graph allows for a detailed spectral analysis as a function of the loop length, due to its exactly solvable nature. To our knowledge, results for the spectrum of graphs with loops are scarce, apart from the analytical formula for the triangular Husimi graph [16].

In this letter we present a systematic study of the spectra of regular Husimi graphs containing undirected or directed edges, going beyond previous studies on local tree-like networks without short loops. We analyze the influence of loops on some important network properties: the size of the spectral gap and the stability of synchronized states. The simplicity and exactness of our equations, confirmed by direct diagonalization methods, leads to accurate results for arbitrary loop lengths and allows for an extension of the Kesten-McKay law to triangular and square undirected Husimi graphs as well as to directed regular graphs without short loops.
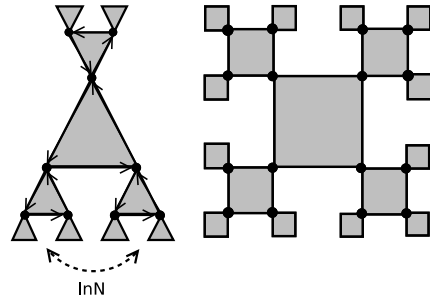

FIG. 1. Local tree-like structure of a $(3,2)$-directed and a $(4,2)$-undirected regular Husimi graph. The average path length between two nodes is of order $\mathcal{O}(\ln N)$.

Sparse regular graphs with loops We consider the ensemble of (ℓ, k)-regular (un)directed Husimi graphs containing N vertices or nodes. Each vertex is incident to $k > 1$ loops composed of ℓ nodes, with k and ℓ independent of N. The indegree and outdegree of any node are equal to each other, and given by $2k$ or k in the case of undirected or directed Husimi graphs, respectively. For $N \to \infty$ the graphs have a local tree-like structure on the level of loops, illustrated in figure 1 for triangular ($\ell = 3$) and square ($\ell = 4$) Husimi graphs. The model allows to interpolate between $\ell = 2$ and $\ell \to \infty$, both cases representing situations where short loops are absent.

We study the spectral density of the $N \times N$ adjacency matrix $\mathbf{J}$ for $N \to \infty$, which is trivially related to the

spectrum of the Laplacian matrix in the case of regular graphs. The matrix element J_{ij} assumes 1 if there is a directed edge from node i to node j, and zero otherwise. Denoting the eigenvalues of a given instance of $\mathbf{J}$ as $\{\lambda_i\}_{i=1,\ldots,N}$, the spectral density is defined as $\rho(\lambda) \equiv \lim_{N\to\infty} \frac{1}{N} \sum_{i=1}^{N} \delta(\lambda - \lambda_i)$. The matrix $\mathbf{J}$ is symmetric or asymmetric depending whether the graph is undirected or directed, respectively. The eigenvalues are real in the former case and complex in the latter. The local tree-like structure shown in figure 1 allows to calculate $\rho(\lambda)$ exactly for $N \to \infty$.

Spectra of undirected Husimi graphs The resolvent $\mathbf{G}(z)$ of $\mathbf{J}$ is defined through $\mathbf{G}(z) \equiv (z - \mathbf{J})^{-1}$, where the complex variable $z = \lambda - i\epsilon$ contains a regularizer ϵ. The spectrum is extracted from the diagonal components of $\mathbf{G}(z)$ according to $\rho(\lambda) = \lim_{N\to\infty,\epsilon\to0^+} (\pi N)^{-1} \mathrm{Im} \mathrm{Tr} \mathbf{G}(\lambda - i\epsilon)$.

Due to the absence of disorder, a closed expression can be derived for the diagonal elements $G_{ii}(z) = G(z)$, $\forall\, i$. For graphs without short loops, either one writes $G_{ii}(z)$ as the variance of a Gaussian function and uses the *cavity method* (or the replica method) [10], or one uses repeatedly the *Schur-complement formula* and the local convergence of graphs to a tree [11]. Generalizing these methods to Husimi graphs [17], we have derived the following equation for $\rho(\lambda)$

$$\rho(\lambda) = \frac{1}{\pi} \lim_{\epsilon\to0^+} \mathrm{Im}[z - k\, G_s]^{-1} \,, \qquad (1)$$

where G_s solves

$$G_s = \mathbb{J}_s^T \Big[\big(z - (k-1)G_s\big)\mathbf{I}_{\ell-1} - \mathbf{L}_{\ell-1} - \mathbf{L}_{\ell-1}^T \Big]^{-1} \mathbb{J}_s \,, \quad (2)$$

with $\mathbf{I}_{\ell-1}$ the $(\ell-1)\times(\ell-1)$ identity matrix, $\mathbf{L}_{\ell-1}$ the $(\ell-1)$-dimensional matrix with elements $[\mathbf{L}_{\ell-1}]_{ij} = \delta_{i,j-1}$, and $\mathbb{J}_s^T$ the $(\ell-1)$-dimensional vector $\mathbb{J}_s^T = (1\ 0\ \ldots\ 0\ 1)$. For $\ell = 2$, the solution of eq. (2) yields the Kesten-McKay law [9], where $\rho(\lambda)$ takes the form

$$\rho(\lambda) = \frac{k}{2\pi} \frac{\sqrt{4(k-1) - \lambda^2}}{k^2 - \lambda^2} \qquad (3)$$

for $|\lambda| < 2\sqrt{k-1}$, and zero otherwise. For $\ell > 2$, we have inverted the matrix in eq. (2) [19], leading to

$$G_s = \frac{2\alpha_{\ell-2} + 2}{\alpha_{\ell-1}} \,, \qquad (4)$$

where the coefficients $\alpha_2, \ldots \alpha_{\ell-1}$ follow from the recurrence relation $\alpha_i = \alpha_1\alpha_{i-1} - \alpha_{i-2}$, with $\alpha_0 = 1$ and $\alpha_1 = z - (k-1)G_s$. Equation (4) leads to a polynomial in the variable G_s and can be solved analytically for smaller values of ℓ, extending the Kesten-McKay law to regular graphs containing short loops. For larger values of ℓ a straightforward numerical solution can be obtained, giving sharp results for $\rho(\lambda)$. Equation (4) is one of the

main results of our work, allowing to compute exactly the spectrum for increasing values of ℓ.

For $\ell = 3$ we recover the analytical expression for $\rho(\lambda)$ presented in [16]. For $\ell = 4$ eq. (4) becomes a cubic polynomial with discriminant

$$D(\lambda) = -\frac{2}{3}\lambda^4 - \frac{\lambda^2}{3}\left(k^2 - 22k + 13\right) + \frac{8}{3}(k-2)^3 \,. \quad (5)$$

Defining the functions $s_\pm(\lambda) = 9\lambda(k+1) - \lambda^3 \pm 9\sqrt{D(\lambda)}$ and $q_\pm(\lambda) = s_+^{1/3} \pm s_-^{1/3}$, the spectrum of square Husimi graphs reads

$$\rho(\lambda) = \frac{6\sqrt{3}\,k\,(k-1)\,q_-(\lambda)}{\pi\Big[2(k-3)\lambda + k\,q_+(\lambda)\Big]^2 + 3\,\pi\,k^2\,q_-^2(\lambda)} \qquad (6)$$

for $D(\lambda) > 0$, and $\rho(\lambda) = 0$ otherwise. The edges of $\rho(\lambda)$ solve the equation $D(\lambda) = 0$. The analytic expression for some higher values of ℓ is given elsewhere [17].

In figure 2 we compare direct diagonalization results of finite matrices with the solution to eq. (4), for $k = 2$ and several values of ℓ. The agreement is excellent, following from the exactness of eq. (4) for $N \to \infty$. When rescaling the matrix elements $J_{ij} \to J_{ij}/\sqrt{2k-1}$ we find analytically the convergence of $\rho(\lambda)$ to the Wigner semi-circle law for $k \to \infty$ and arbitrary ℓ [18]. Interestingly,
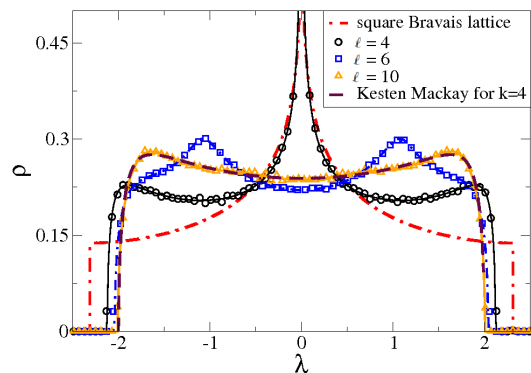

FIG. 2. Spectrum of (ℓ, k) undirected Husimi graphs with $k = 2$ and $J_{ij} \to J_{ij}/\sqrt{2k-1}$, obtained by solving eqs. (1) and (4). The symbols are direct diagonalization results of adjacency matrices of size $N = 10^4$. The spectrum of the two-dimensional square Bravais lattice and the Kesten-McKay law are presented for comparison.

the spectrum of a square Husimi graph exhibits a striking similarity with the spectrum of the two-dimensional square Bravais lattice [20], with the appearance of a power-law singularity at $\lambda = 0$ with $\rho(\lambda) \sim |\lambda|^{-1/3}$. In the case of the square Bravais lattice, the spectral density contains a Van Hove singularity at $\lambda = 0$, with a logarithmic divergence. Our results thus suggest that Van Hove singularities are related to the local neighborhoods and

not to the dimensional nature of lattices [20]. For $\ell \to \infty$, the spectrum converges to the Kesten-McKay law with degree $2k$ [9], as illustrated in figure 2 for $\ell = 10$. Therefore, loops composed of ten nodes can be neglected and the graph can be considered locally tree-like [10, 11].

Spectra of directed Husimi graphs In the case of directed Husimi graphs, the density of states $\rho(\lambda)$ at a certain point $\lambda = x + iy$ of the complex plane can be written as $\rho(\lambda) = \lim_{N\to\infty}(N\pi)^{-1}\partial^*\mathrm{Tr}\mathbf{G}(\lambda)$, where $\partial^* = \frac{1}{2}\left(\frac{\partial}{\partial x} + i\frac{\partial}{\partial y}\right)$ and $\mathbf{G}(\lambda) = (\lambda - \mathbf{J})^{-1}$. The operation $(\cdot)^*$ denotes complex conjugation. Due to the non-analytic behavior of $G_{ii}(\lambda)$ in the complex plane [21], it is convenient to define the $2N \times 2N$ block matrix [22]

$$\mathbf{H}_\epsilon(\lambda) = \begin{pmatrix} \epsilon\mathbf{I}_N & -i(\lambda - \mathbf{J}) \\ -i(\lambda^* - \mathbf{J}^T) & \epsilon\mathbf{I}_N \end{pmatrix}. \qquad (7)$$

The $N \times N$ lower-left block of $\lim_{\epsilon\to 0^+} \mathbf{H}_\epsilon^{-1}(\lambda)$ is precisely the matrix $\mathbf{G}(\lambda)$. Thus, the problem reduces to calculating the matrix elements $\mathcal{G}_j(\lambda, \epsilon) = \left[\mathbf{H}_\epsilon^{-1}(\lambda)\right]_{j+N,j}$ $(j = 1, \dots, N)$, from which the spectrum is determined according to $\rho(\lambda) = -\frac{i}{N\pi}\lim_{N\to\infty, \epsilon\to 0^+}\sum_{j=1}^N \partial^*\mathcal{G}_j(\lambda, \epsilon)$.

By representing $\left[\mathbf{H}_\epsilon^{-1}(\lambda)\right]_{j+N,j}$ as a Gaussian integral one can generalize the cavity method, as developed for sparse non-Hermitian random matrices [22], to calculate the spectrum of directed Husimi graphs [17]. Due to the absence of disorder we have that $\mathcal{G}_j(\lambda, \epsilon) = \mathcal{G}(\lambda, \epsilon)$, $\forall j$, and $\rho(\lambda)$ is given by

$$\rho(\lambda) = \frac{1}{i\pi}\lim_{\epsilon\to 0} \partial^* \left[\mathbf{S}_\epsilon(\lambda) + k\,\mathbf{G}_A\right]_{21}^{-1}, \qquad (8)$$

where $\mathbf{S}_\epsilon(\lambda) = \left[\epsilon\mathbf{I}_2 - i\left(x\sigma_x - y\sigma_y\right)\right]$ and (σ_x, σ_y) are Pauli matrices. For $\ell > 2$, the two-dimensional matrix $\mathbf{G}_A$ solves the equation

$$\mathbf{G}_A = \mathbb{J}_A^T\Big[\left(\mathbf{S}_\epsilon(\lambda) + (k-1)\mathbf{G}_A\right) \otimes \mathbf{I}_{l-1}$$
$$+ i\mathcal{J} \otimes \mathbf{L}_{\ell-1} + i\mathcal{J}^T \otimes \mathbf{L}_{\ell-1}^T\Big]^{-1}\mathbb{J}_A, \qquad (9)$$

where $\mathbb{J}_A^T$ is the $2 \times 2(\ell - 1)$ block matrix $\mathbb{J}_A^T = (\mathcal{J}\ 0 \dots 0\ \mathcal{J}^T)$, with $\mathcal{J} = \frac{1}{2}(\sigma_x + i\sigma_y)$. The derivative of eq. (9) yields an equation in $\partial^*\mathbf{G}_A$, which has to be solved together with (8) to find $\rho(\lambda)$. Equation (9) allows to derive sharp numerical results for the spectrum of directed Husimi graphs as a function of ℓ.

In figure 3 we present the spectrum $\rho(\lambda)$ for $\ell = 3$ and $k = 2$, comparing the solution to eqs. (8-9) with direct diagonalization results. The agreement is excellent. A prominent feature of $\rho(\lambda)$ is the ℓ-fold rotational symmetry, due to the transformation properties of $\mathbf{G}_A$ under rotations of $2\pi/\ell$. By rescaling $J_{ij} \to J_{ij}/\sqrt{k-1}$, we find analytically the convergence of $\rho(\lambda)$ to Girko's circular law for $k \to \infty$ and arbitrary ℓ [18].

Analogously to undirected Husimi graphs, $\rho(\lambda)$ converges to the spectrum of a directed regular graph without short loops for $\ell \to \infty$. In this case, we find a remarkable extension of the Kesten-McKay law, Eq. (3),
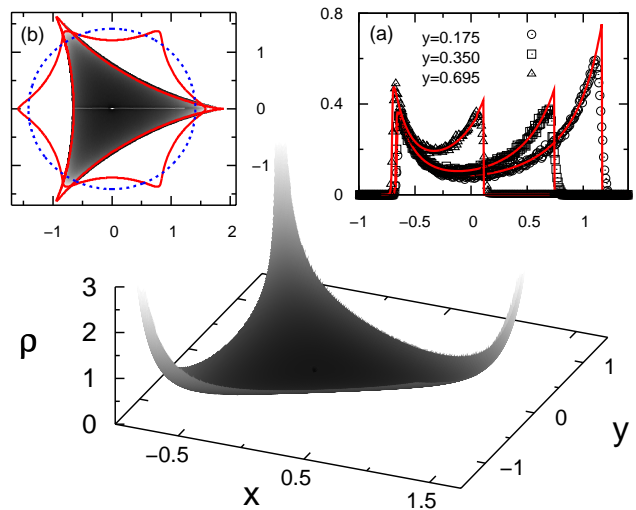

FIG. 3. Spectrum of directed Husimi graphs with $\ell = 3$ and $k = 2$, obtained from eqs. (8-9). Inset (a) shows three cuts along the real direction (red curves), together with direct diagonalization results (symbols) obtained from an ensemble of 3×10^4 matrices of size $N = 10^3$. Inset (b) shows theoretical results for the boundary of $\rho(\lambda)$ for $\ell = 3$ and $\ell = 6$ (red curves). The number of corners in each boundary is equal to the value of ℓ and the blue dashed curve corresponds to the circle $|\lambda|^2 = k$, for $\ell \to \infty$. For comparison, direct diagonalization results are also shown in grey scale for $\ell = 3$.

to directed graphs, where $\rho(\lambda)$ takes the form

$$\rho(\lambda) = \frac{k-1}{\pi}\left(\frac{k}{k^2 - |\lambda|^2}\right)^2, \qquad (10)$$

for $|\lambda|^2 < k$, and zero otherwise. A comparable equation appeared in [23], but with a different support of $\rho(\lambda)$.

In inset (b) of figure 3 we plot the boundary of $\rho(\lambda)$ for $k = 2$ and increasing values of ℓ. In accordance with eq. (10), the boundary converges to the circle $|\lambda|^2 = k$ in the limit $l \to \infty$. For $\ell = 10$ we have obtained numerically that $\rho(\lambda)$ is given approximately by eq. (10) and the graph becomes locally tree-like [22].

Structural and dynamical properties Let us order the eigenvalues of a regular undirected Husimi graph as $\lambda_1 < \lambda_2 < \cdots < \lambda_N$, where $\lambda_N = 2k$. The *spectral gap* g and the *eigenratio* Q are, respectively, defined by $g \equiv (\lambda_N - \lambda_{N-1})/2k$ and $Q \equiv (\lambda_N - \lambda_1)/(\lambda_N - \lambda_{N-1})$. Analogously, for regular directed Husimi graphs, the eigenvalues can be ordered according to their real parts $\mathrm{Re}\lambda_1 < \mathrm{Re}\lambda_2 < \cdots < \mathrm{Re}\lambda_N$, with $\mathrm{Re}\lambda_N = k$. In this case, the spectral gap g and the eigenratio Q are given by $g \equiv (\mathrm{Re}\lambda_N - \mathrm{Re}\lambda_{N-1})/k$ and $Q \equiv (\mathrm{Re}\lambda_N - \mathrm{Re}\lambda_1)/(\mathrm{Re}\lambda_N - \mathrm{Re}\lambda_{N-1})$.

The spectral gap g controls the speed of convergence to the stationary state of diffusion processes on the graph [1]. Designing communication networks with a large g is known to be important due to improved robustness and communication properties [2, 3], for undirected networks. The eigenratio Q measures the propensity for

synchronization in networks of oscillators [4, 5]. A linear stability analysis shows that synchronized states are more stable for smaller values of Q.

Figure 4 depicts g and Q as functions of ℓ for regular Husimi graphs, showing that g increases while Q decreases for increasing values of ℓ. For undirected Husimi graphs, g and Q converge, respectively, to $(k - \sqrt{2k-1})/k$ and $2k/(k - \sqrt{2k-1})$ as $\ell \to \infty$, consistent with the Alon-Boppana bound for the second largest eigenvalue [24]. For directed Husimi graphs g and Q converge to $(k - \sqrt{k})/k$ and $2k/(k - \sqrt{k})$, respectively. In summary, short loops have a negative influence on the synchronization properties and on the size of the spectral gap, which is more pronounced at low connectivities.
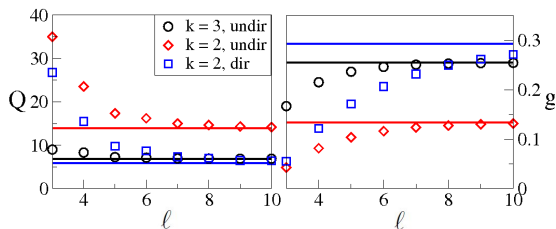

FIG. 4. Spectral gap g and eigenratio Q of Husimi graphs as functions of ℓ for different values of k, with the asymptotic behavior for $\ell \to \infty$ indicated by solid lines.

Conclusions We have determined the spectrum of sparse regular random graphs with short loops through a set of exact equations, including extensions of the Kesten-McKay law to triangular and square undirected Husimi graphs as well as to directed regular graphs without short loops. We find that short loops in directed and undirected networks have a negative influence on the stability of synchronized states, they also worsen the communication properties due to a decrease of the spectral gap. Our spectral results make the absence of loops in network construction apparent [5], while neural networks are under-short looped [14]. For the square Husimi graph we recover a singularity at the origin, which is also present in a square Bravais lattice. Overall, we find that the spectra of Bravais lattices are similar to the spectra of Husimi graphs with suitable neighborhoods, indicating that Husimi graphs serve as good toy models for Bravais lattices. Our results on spectra of sparse random matrices are of wide interest to diverse fields including the study of Markov chains [25], dynamics of spin-glasses [26], etc. Since our work is mainly based upon the cavity method, it allows for an extension to e.g. irregular graphs with loops [10] and eigenvector localization studies [27].

[1] A. Barrat, M. Barthélemy, A. Vespignani, *Dynamical processes on networks*, Cambridge University Press (2008); M. E. J. Newman, *Networks, An Introduction*, Oxford University Press (2010).

[2] S. Hoory, N. Linial, A. Wigderson, Bull. Amer. Math. Soc. **43**, 439 (2006).

[3] M. R. Murty, J. Ramanujan Math. Soc. **18**, 1 (2003).

[4] M. Barahona, L. M. Pecora, Phys. Rev. Lett. **89**, 054101 (2002).

[5] L. Donetti, P. I. Hurtado, M. A. Muñoz, Phys. Rev. Lett. **95**, 188701 (2005); T. Nishikawa, A. E. Motter, Phys. Rev. E **73**, 065106 (2006).

[6] L. Lovász, P. Winkler, *Mixing of random walks and other diffusions on a graph*, Cambridge University Press (1995), 119-154.

[7] F. R. K. Chung, *Spectral Graph Theory*, American Mathematical Society (1997); B. Georgeot, O. Giraud, D. L. Shepelyansky, Phys. Rev. E **81**, 056109 (2010); Z. Wang, A. Scaglione, R. Thomas, IEEE Transactions on Smart Grid **1**, 1949-3053 (2010).

[8] B. Bollobás, *Random graphs*, Cambridge University Press (2001).

[9] H. Kesten, Trans. Amer. Math. Soc. **92**, 336354 (1959); B. D. McKay, Linear Algebra Appl. **40**, 203-216 (1981).

[10] T. Rogers, K. Takeda, I. P. Castillo and R. Kühn, Phys. Rev. E. **78**, 031116 (2008); R. Kühn, J. Phys. A: Math. Theor. **41**, 295002 (2008).

[11] C. Bordenave, M. Lelarge, Random Structures and Algorithms **37**, 332 (2010).

[12] J. Fortin, J. Phys. A: Math. Gen. **38**, L57 (2005); A. N. Samukhin, S. N. Dorogovtsev, J. F. F. Mendes, Phys. Rev. E **77**, 036115 (2008); I. J. Farkas, I. Derényi, A.-L. Barabási and T. Vicsek, Phys. Rev. E, **64**, 026704 (2001); R. Kühn, J. Mourik, J. Phys. A: Math. Theor. **44**, 165205 (2011).

[13] P. M. Gleiss et al., arxiv:cond-mat/0009124 (2000); G. Bianconi, G. Caldarelli, A. Capocci, Phys. Rev. E **71**, 066116 (2005).

[14] G. Bianconi, N. Gulbahce, A. E. Motter, Phys. Rev. Lett. **100**, 118701 (2008).

[15] K. Husimi, J. Chem. Phys. **18**, 682-684 (1950); F. Harary, G. Uhlenbeck, PNAS **39**, 315-322 (1953).

[16] M. Eckstein, M. Kollar, K. Byczuk and D. Vollhardt, Phys. Rev. B **71**, 235119 (2005); M. Galiceanu, A. Blumen, J. Chem. Phys. **127**, 1349004 (2007).

[17] F. L. Metz, I. Neri, D. Bollé, in preparation.

[18] Z. D. Bai, J. W. Silverstein, *Spectral Analysis of Large Dimensional Random Matrices*, Science Press (2006).

[19] Y. Huang, W. F. McColl, J. Phys A: Math. Gen. **30**, 7919 (1997).

[20] P. Fazekas, *Lecture notes on Electron Correlation and Magnetism*, World Scientific (1999).

[21] J. Feinberg, A. Zee, Nucl. Phys. B **504**, 579 (1997).

[22] T. Rogers and I. P. Castillo, Phys. Rev. E **79**, 012101 (2009).

[23] T. Rogers, *New results on the spectral density of random matrices*, thesis (2010).

[24] N. Alon, Combinatorica **6**, 83 (1986); J. Friedman, Mem. Amer. Math. Soc. **195**, 910 (2008).

[25] J. R. Norris, *Markov Chains, Statistical and Probabilistic Mathematics*, Cambridge University Press (1998).

[26] G. Semerjian and L. F. Cugliandolo, Europhys. Lett. **61**, 247 (2003).

[27] G. Biroli, G. Semerjian, M. Tarzia, Prog. Theor. Phys. Suppl. **184**, 187 (2010); F. L. Metz, I. Neri, D. Bollé, Phys. Rev. E **82**, 031135 (2010).